Comparison of nanoindentation results obtained with Berkovich and Cube Corner indenters

Thomas Chudoba, Patrick Schwaller, R. Rabe, J.-M. Breguet, Johann Michler

▶ **To cite this version:**

HAL Id: hal-00513706

https://hal.archives-ouvertes.fr/hal-00513706

Submitted on 1 Sep 2010

Comparison of nanoindentation results obtained with Berkovich and Cube Corner indenters

Comparison of nanoindentation results obtained with Berkovich and Cube Corner indenters

T. Chudoba*[1], P. Schwaller[2], R. Rabe[2, 3], J.-M. Breguet[3], J. Michler[2]

[1] ASMEC GmbH, D-01454 Radeberg, Germany

  E-Mail: t.chudoba@asmec.de

[2] Materials Technology Laboratory, Empa, Materials Science and Technology, CH- 3602
  Thun, Switzerland

[3] Institut de Production et Robotique, IPR-LSRO, EPF Lausanne, CH-1015 Lausanne-EPFL,
  Switzerland

Abstract

There is increasing interest in using sharp cube corner indenters in nanoindentation experiments to study plastic properties. In combination with finite element methods it is for instance possible to extract stress-strain curves from load-displacement curves measured with differently shaped pyramidal indenters. Another example is the fracture toughness of coatings, which can be studied using cracks produced during indentation with cube corner tips. We have carried out indentation experiments with Berkovich and cube corner indenters on eight different materials with different mechanical properties. To gain information about the formation of pile-up and cracks, indentation experiments with cube corner indenter were performed inside a Scanning Electron Microscope (SEM) using a custom-built SEM-Microindenter. The results show that reliable hardness and modulus values can be measured using cube corner indenters. However, the fit range of the unloading curve has a much bigger influence on the results for the cube corner than for the Berkovich tip. The unloading curves of a cube corner measurement should therefore be carefully inspected to determine the region of smooth curvature and the unloading fit range chosen warily. Comparison of the modulus results shows that there is no significant difference between cube corner and Berkovich measurements. Also for hardness, no fundamental difference is observed for most of the investigated materials. Exceptions are materials like silicon nitride, cemented carbide or glassy carbon, where a clear difference to the hardness reference value has been observed although the modulus difference is not pronounced.

* Corresponding author: t.chudoba@asmec.de

1. Introduction

Nanoindentation is nowadays an established tool for the measurement of hardness and Young's modulus of surfaces and thin films. In the thin film community the use of three-sided Berkovich pyramids as indenters became a standard in contrast to four-sided Vickers pyramids that are mostly used in conventional hardness tests. The reason for this preference is the possibility to prepare sharper tips with smaller tip rounding. Vickers indenters may show the so called "chisel edge" where the four faces don't meet each other in one single point. This results in asymmetrical impressions, especially for small indents, and complicates the determination of an accurate area function. Another indenter with the shape of a three-sided pyramid is the cube corner. A diamond cube is simply used in such a way that the indentation direction is along the space diagonal which connects opposite corners. This indenter with a face angle (angle between surface normal of sample and indenter face) of 35.3° is much sharper than a Berkovich pyramid with a face angle of 65.3°. Radial cracks, which normally start at the corners of the pyramid, are therefore easier to induce. These cracks can be used for the investigation of the fracture toughness of coatings (see [1, 2]). However, for the measurement of hardness and Young's modulus cracks are undesirable since they may cause measurement errors.

In recent years there has been, however, a growing interest to use cube corner indenters as an alternative indenter type to study plastic properties. Due to the self-similarity of pyramidal indenters it is not possible to realize different strain states with one and the same tip. Beside the very first depth range where the tip rounding plays a role, the stress field is growing but keeping the same stress ratio with the increasing contact area. This disadvantage can be overcome by using tips with different face angles. Stauss et al. and Bucaille et al. [3,4,5] have shown, by using Berkovich and cube corner indenters combined with finite element calculations the same stress-strain values as in tensile tests can be obtained with this method. Chollacoop et al. [6] have applied a similar method with Berkovich and 60° cone tips. Field et al. performed indentations on fused silica and glassy carbon with different tip geometries including Berkovich and cube corner for the determination of the fracture toughness [7]. In this study the hardness and modulus values were however not determined from the indentation data but taken from the literature.

Little work has been done, however, to use cube corner indenters to measure Young's modulus and hardness in the same way as Berkovich indenters and to check the applicability of the Oliver and Pharr analysis method [8]. Generally it is expected that the much sharper

cube corner tip deforms the material more by a cutting mechanism and results in a stronger pile-up. Such an upward flow of material can be described the slip-line theory, developed originally in two dimensions by Hill [9]. By comparison, the plastic zone of a blunt Berkovich tip is constrained by the surrounding material and upwards flow of material is only possible if the radial expansion of the plastic zone is big enough. It is assumed that the displaced volume is taken up entirely by elastic strains within the specimen material. This deformation mechanism can be described by the expanding cavity models of Marsh [10] and Johnson [11]. The transition range between the two models is not well defined and depends on the material and the friction coefficient between indenter and sample. Therefore it is possible that Berkovich as well as cube corner indents can be described with the same model. Zhang and Sakai [12] investigated geometrical effects of pyramidal indenters with different face angles on the elastoplastic contact behaviors of ceramics and metals. They found different hardness results depending on the face angle; however their results cannot be compared to ours because they calculated the hardness values with a model which assumes a quadratic behavior of the unloading curves which we did not observe for any of our investigated materials. Further they tried to derive a face angle independent "true" hardness value that was related to the flow stress by a constraint factor C. Indeed, H=C*Y is the well known Tabor relation for metals [13] with a constraint factor of about 3 for a representative strain of 8%. According to this model hardness should only weakly depend on the face angle.

We have carried out indentation experiments with Berkovich and cube corner indenters on eight different homogeneous materials with two different commercial nanoindentation instruments (UMIS-2000, CSIRO, Australia and Nanoindenter XP, MTS, USA). A large load range between 0.3 mN and 500 mN was used to obtain depth dependent results. Fused silica and sapphire were used as reference materials for a careful determination of the compliance of the two instruments and the indenter area functions. Finally hardness and modulus results were calculated according to ISO 14577 part 1 [14] and compared. The results are discussed in relation to reference values obtained with other measurement methods. To gain information about the formation of pile-up and/or crack formation with cube corner indenters, additional indentation experiments were performed inside a Scanning Electron Microscope (SEM) using a custom-built SEM-Microindenter (for details see [15]) using the same tip as for the MTS Nanoindenter XP measurements.

2. Experimental

2.1. Material selection

Eight materials covering a wide range of mechanical properties were investigated in this study. The reference values for the hardness and the Young's modulus of these materials are listed in table 1. Most of the samples were also used in the European project "Certified Reference Materials for Depth Sensing Indentation Instrumentation" (DESIRED) [16] which was finished in February 2004. The Ni sample was already investigated and used as substrate in the European project INDICOAT [17]. A special ultra-fine grain cemented carbide (hardmetal) sample was delivered by the company Widia, Germany. In contrast to conventional cemented carbide the grain size of the WC particle was in the order of 100 nm and the cobalt content was very low. The distribution of the WC particles in this sample was highly homogeneous and its Young's modulus close to the value of pure WC.

The conventional Vickers hardness and the Young's modulus of the materials were determined independent of the nanoindentation experiments as reference values. The results are given in table 1. Vickers hardness tests have been carried out by trained operators at the Federal Institute of Materials Research and Testing (BAM) in Berlin with a Reichert-Jung Micro-Duromat 4000. The magnification of the optical system was 1000 x. Both diagonals of the indents were measured and average length was determined. A load of 500 mN was applied in 30 s and the hold period at maximum load was 12 s. The instrument is part of a quality control system according to ISO 17025. The calibration is checked every half-year according to DIN 51220 with the help of a hardness reference block with 315 ± 10 HV 0.1 and 333 ± 24 HV 0.015.

Ten measurements were done on every sample and the Vickers hardness results were averaged. The equivalent H_{IT} value was estimated using the informative relationship given in ISO 14577: $H_{IT} = HV/0.0945$. Table 1 gives the hardness H_{IT} and additionally the standard deviation of the hardness results σ_H.

The Young's modulus of fused silica was measured within the INDICOAT project [17] with different methods (Laser Surface Acoustic Wave, Acoustic Microscopy, Brillouin scattering). The moduli of the Au-Cu alloy (containing 18% Cu), Si_3N_4 and cemented carbide (hardmetal) were measured with surface acoustic waves at the BAM and the Fraunhofer Institute IWS in Dresden, Germany. The moduli of W and Ni are literature data [18]. The modulus of Sigradur glassy carbon is an average value from indentation measurements done with different instruments and loads. The modulus of sapphire was calculated as a weighted elastic average on basis of the single crystal elastic constants for hexagonal symmetry. The sapphire surface

had a (0001) orientation. Perpendicular to this basal plain in the direction of indentation is the absolute modulus maximum with E = 461 GPa. Directions within the (0001) plain have a modulus of about 380 GPa which was confirmed by surface acoustic wave measurements. The modulus average over the whole space is 404.7 GPa. The indentation direction with the highest modulus is higher weighted than the other directions and the effective modulus is therefore slightly higher than the average with about 420 GPa.

2.2. Nanoindentation measurements

The experiments were carried out with an UMIS-2000 Nanoindenter (CSIRO, Australia) at the Technical University of Chemnitz, Germany and a Nanoindenter XP (MTS, Knoxville, USA) at EMPA in Thun, Switzerland. A measurement cycle consisted of a loading segment, followed by a first hold period at constant maximum load to reduce creep effects which could influence the shape of the unloading curve. The unloading segment was followed by a second hold period at about 10% of the maximum load for the determination of the thermal drift of the instrument. Different loading and unloading times were used depending on the maximum load and the instrument. A typical total measurement time for the UMIS was 400 s and for the Nanoindenter XP 140 s. The loading time of the UMIS depends on the number of data points and cannot be varied markedly. In contrast to the Nanoindenter XP, which used a linear force increase and decrease over time, the force steps followed a quadratic rule. The hold period at maximum load was set to 30 s for the XP and between 30 s and 60 s for the UMIS. The second hold period at the end of the measurement cycle was 60 s for the XP and 45 s for the UMIS. Only the last 30 s were used for both instruments to apply a linear fit and to determine the thermal drift rate. This was possible with an accuracy of 0.003 nm/s for the UMIS, and 0.005 nm/s for the XP, respectively.

The true surface position was determined by a correction procedure that uses a fit of the first displacement data points after contact for a back-extrapolation to zero depth. The fit was done assuming a Hertzian contact for the first part of the loading segment (typically below 30 nm depth). The zero point correction is necessary for the UMIS because the instrument software only recognizes the surface if the contact force exceeds about 5-10 µN. The deformation at this force and the influence of surface roughness can result in a zero shift of more than 3 nm. This would influence the results markedly when the absolute deformation was small. The determination of the zero position of the displacement axis could also be improved by this

method for the XP although it uses another principle for the surface detection. More details can be found in [19].

Between 8 and 10 different loads within a range between 300 µN and 500 mN were used to measure the reference materials fused silica and sapphire. For the other materials at least 5 different loads (5 mN, 30 mN, 100 mN, 300 mN and 500 mN) were applied with the XP. UMIS measurements were carried out with some additional loads of 300 µN, 1 mN, 3 mN and 50 mN. 10 indentations separated by a distance of 50 µm were made for each load on every sample and average load-displacement curves were calculated. Finally, the averaged depth values were corrected for the instrument compliance at the corresponding load and analyzed. This is in contrast to the usual analysis of every single curve and reduces the uncertainty of the data due to the averaging. Additionally, it reduces the amount of data to be handled. A pop-in event would be smeared out in such an average curve but this is not a problem here because such effects were not included in this work. Chudoba has shown in previous work [17] that the results of this procedure agree well with the hardness or modulus average of the results from every single curve if the curves are smooth.

The data analysis for both instruments, including all corrections, was done with the instrument independent software IndentAnalyser® (ASMEC GmbH, Radeberg, Germany).

2.3. Determination of the instrument compliance

An accurate knowledge of the instrument compliance is indispensable for calculating reliable hardness and Young's modulus values from load-displacement curves, especially at higher loads. We determined the instrument stiffness by a comparison of the area functions obtained using data of two different materials (fused silica and sapphire). The measurements were done using a Berkovich tip and the same stiffness function was used for the evaluation of cube corner data. Because the influence of the instrument stiffness becomes more important for samples with a high modulus, it is recommended to include a material with a high modulus (sapphire) for the instrument stiffness determination. In the following, the procedure for the determination of the instrument stiffness is described in detail:

First 10 load-displacement curves for fused silica and sapphire with different nominal maximum loads (500, 300, 100, 50, 30, 10, 5, 3, 1, 0.5, and 0.3 mN, respectively) were measured. From the average curves the effective maximum load F, the unloading stiffness S, the maximum depth h_{max}, the depth after unloading h_0, and the unloading exponent m were determined. It is important to note that these quantities (with the exception of m) were obtained from the load-displacement curve without a correction of instrument compliance.

The instrument compliance C_f was determined such that the area functions obtained from both reference materials agree. This was done under the assumption that the compliance C_f is the only parameter responsible for the difference in the area function. The contact depth h_c is related to C_f according to

$$h_c = h_{max} - \frac{F}{S_f} - \varepsilon(m) \cdot F \cdot (C - C_f)$$ (1)

ε describes the ratio between the elastic deformation above and below the contact area. There is an unequivocal relation between ε and the unloading exponent m (see for instance [20]). $\varepsilon=1$ belongs to m=1 (flat punch indenter geometry); $\varepsilon=0.75$ belongs to m=1.5 (sphere) and $\varepsilon=0.727$ to m=2 (cone). For real materials after plastic deformation ε may vary according to a complicated function between 0.7 and 0.8.

The square root of the contact area A_C is given by

$$\sqrt{A_C} = \frac{\sqrt{\pi}}{2} \frac{1}{E_r} \frac{1}{C - C_f} (1 + u_r)$$ (2)

where E_r is the reduced modulus

$$\frac{1}{E_r} = \frac{1 - \nu_i{}^2}{E_i} + \frac{1 - \nu_s{}^2}{E_s} \tag{3}$$

u_r is the radial displacement correction;

$$u_r = \frac{(1 - 2\nu)(1 + \nu)}{2} \frac{F}{E_r \cdot a^2} \cos(\arctan(\frac{h_0}{a})) \tag{4}$$

h_0 is the residual depth, and a is the equivalent contact radius

$$a = \sqrt{\frac{A_c}{\pi}} \tag{5}$$

The additional radial displacement correction which is not included in ISO standard 14577 [14], and allows for elastic displacement within the surface plane. Although the lateral elastic displacement in indentation experiments has already been estimated by Johnson [11] and others it is normally not considered on the assumption that it can be neglected. In contrast to Johnson's result for fully elastic deformation with a spherical indenter, equation (4) is also valid for additional plastic deformation.

Sometimes an additional geometrical factor $1/\beta$ is incorporated in eq. (2) in order to account for the non-rotational symmetric shape of the pyramids. However all calculations in the literature (for instance [21] or [22]) were done for the fully elastic case and gave values between 1.02 and 1.14 for the Berkovich indenter. For elastoplastic deformations the infinite elastic stresses at edges and tip will be reduced drastically by the plastic displacement of material. It is well known that the plastic zone of pyramidal indentations is approximately rotationally symmetric (see for instance [11]) and that the elastic field after plastic deformation has a similar shape. For this reasons, no value is given or recommended for beta in the standard ISO 14577 and it is indeed better to use beta = 1 for pyramidal tips.

The Young's modulus E and Poisson's ratio values ν of both indenter (index i) and sample (index s) were assumed to be known. We took the following values for the calculations: For diamond (E = 1140 GPa, ν = 0.07), for fused silica (E = 72 GPa, ν = 0.17), and for sapphire (E = 420 GPa, ν = 0.24), respectively.

To begin with, the instrument stiffness was set to infinite. As already mentioned, the instrument stiffness has a larger influence on the measurement of a material with a higher modulus. Therefore the $\sqrt{A}(h)$-curve for the stiffer material lies below the curve of the other and the resulting square root of the contact area, according to equation (2), changes more with varying instrument stiffness than for the less stiff material. At a certain instrument stiffness value both curves meet each other. The procedure was therefore to decrease the instrument

stiffness stepwise decreased from 10^6 mN/µm until both area functions agreed as closely as possible. This was done for both area functions with the formulas given above. A relatively complicated iterative procedure is repeated six times to get, finally, a force dependent stiffness function. Stiffness results for forces below 30 mN were ignored because the accuracy of the stiffness in this range is normally not good enough. Below 30 mN constant instrument stiffness was assumed. The mean instrument compliance (inverse stiffness) of the UMIS-2000 was 0.21 nm/mN. It was slightly increased towards smaller forces up to 0.286 nm/mN. The mean compliance of the Nanoindenter XP was 0.15 nm/mN. It increased to 0.16 nm/mN at 30mN.

2.4. Determination of indenter area function

The area function $A(h_c)$ for the Berkovich indentation tip was calculated with the same measurement data of fused silica and sapphire, and with the same formulas (see above) as was used for the stiffness calibration. The compliance function as determined before, was used for all calculations. The calculations were done according to the ISO 14577 standard but allowed, in addition, a variable ε factor and a radial displacement correction u_r as mentioned above. This is a refinement of the ISO standard method and it improves the accuracy of the analysis by some percent. The influence of these corrections depends on the material. They have the largest influence on fused silica. The increase in the value of the square root of A_C calculated by equation (2) is about 5% for the Berkovich indenter. This results in a 5% reduction in the modulus and a 10% reduction in the hardness, because hardness scales with $1/A_C$. The increase of $\sqrt{A_C}$ is the smallest for Ni at only 0.25%. Fused silica has (with $m = 1.2$ for Berkovich) the smallest unloading exponent of all investigated materials. The standard epsilon value of 0.75 is only absolutely correct for an unloading exponent of 1.5. An unloading exponent of 1.2 corresponds to an epsilon value of 0.8 and increases the square root of A_C for fused silica by 2.3%. In contrast, sapphire has an unloading exponent of about 1.5 and the correction has no influence for this material.

For the Berkovich measurements, a fit range of the unloading curve between 98% and 40% of the maximum load F_{max} was used. The same values for E and ν as indicated in the previous section were used. It turned out that these parameters did not yield good results for the calibration of the cube corner tip with fused silica. In contrast to the Berkovich tip, for the cube corner tip, it could be seen that a kink occurs in the unloading curves at about 50% unloading. A fit with a power function gave an unloading exponent of about 1.4 if the fit range was restricted to the data above the kink. Otherwise the unloading exponent was two or higher. To avoid this kink influencing the accuracy of the fit of the unloading curve in the evaluation of cube corner data, a reduced range, between 98% and 50% of the unloading curve, was used for the curve fit.

A second aspect to consider was the reference value of the Young's modulus for the sapphire sample. In contrast to the other materials investigated in this work, the single-crystalline sapphire sample is elastically anisotropic and has six independent elastic constants (see for instance Wachtmann [23] and Vlassak [24]). Due to the different indentation shapes induced by plastic deformation with Berkovich and cube corner indenters, the contributions of the various crystallographic directions around the indent to the absolute elastic response may be different. We mentioned that the influence of the stiffest direction perpendicular to the (0001)

surface plane is less pronounced for the sharper cube corner tip. For cube corner data the best calibration was obtained by using a modulus of 408 GPa instead of the 420 GPa value found for the Berkovich indenter. This is closer to the isotropic average of 405 GPa.

The tip rounding of the UMIS Berkovich, a much used tip, was much bigger than that of the Nanoindenter XP. The tip radius of the UMIS Berkovich was determined to be about 0.84 µm while the radius of the XP Berkovich and the cube corner indenter was about 0.25 µm and less than 0.15 µm, respectively. The radius was obtained from an elastic fit of the load-displacement curve in the very low load range using the Hertzian model. The large tip radius of the UMIS tip has an effect on the hardness results at small loads, as is shown below. The different tip radius also influences the maximum indentation depth. For example sapphire measurements at 10 mN with the UMIS Berkovich were purely elastic with a maximum depth of 86 nm. The same measurements with the XP Berkovich and cube corner indenters were plastic and reached indentation depths of 141 nm and 336 nm, respectively. In this example the sharper cube corner tip gives rise to a 2.4 times larger indentation depth. This illustrates the much higher strain induced with the cube corner indenter.

3. Results and Discussion

3.1. Influence of the unloading fit range

Figure 1 shows the Young's modulus values obtained from Berkovich (squares) and cube corner (triangles) data measured for fused silica (Fig. 1a), sapphire (Fig. 1b) and Sigradur glassy carbon (Fig. 1c). The maximum load for fused silica and glassy carbon was 500 mN, for sapphire 100 mN. Higher applied loads for sapphire led to crack formation with large pop-in events in the load displacement curves. Different ranges of the unloading curve have been fitted. The upper fit limit was set to 100% of the maximum load F_{max}, the lower limit varied between 80% and 10% of F_{max}. A fit range of 90% from F_{max} represents a fit from 100% down to 10% of F_{max}. Therefore the fit range increases from left to right in Fig. 1. The horizontal solid lines indicate the reference Young's modulus values (see Table 1) obtained with other methods. As can be deduced from the graphs of Fig. 1 the modulus values calculated from Berkovich measurements are almost unaffected by a variation of the unloading fit range and the experimental values are in fair agreement with the reference values. For cube corner data however, a strong influence of the fit range is evident. For fused silica and sapphire an increase in the modulus result is observed with increasing fit range. Note that for both materials the values closest to the reference are obtained for a lower fit limit between 50 and 60% of F_{max}, a range which was used in the following for the data evaluation of all loads. For glassy carbon the modulus decreases with increasing fit range. Only for a fit between 100% and 80% F_{max} can the reference value be obtained. The reason for this can be found by a closer look at the unloading curve (not shown here). There is a distinct kink in the cube corner curve after unloading to 80% F_{max} (F = 400 mN). Therefore only the upper 20% data were used for the fit of the unloading curve of glassy carbon in the following data analysis. The reason for the kink is not clear. Possibly it is connected with first cracking. Cracks parallel to the surface can be seen in the SEM images (see Fig. 3).

A similar but less pronounced kink can be seen in the unloading curves of fused silica at 50% F_{max} as mentioned previously. These kinks were nearly independent of the maximum load down to about 10mN. The results show that the unloading fit range is a critical issue for cube corner data analysis. The unloading curves should be carefully inspected for a smooth curvature. Instead of the recommended 80% fit range for Berkovich or Vickers indenters in [14], a fit range of less than 50% should be preferentially used to get comparable results.

3.2. Modulus results

The results of all measurements are summarized in Table 1. All values for one material obtained at different loads were averaged. Hardness results below 40 nm contact depth, however, were not considered in the average to exclude the influence of tip rounding. The indicated errors are the standard deviations obtained from the different loads without considering the scatter of ten measurements performed at one load. This standard deviation represents therefore the homogeneity of the materials over the depth.

Fig. 2 shows the depth dependent modulus results of all investigated materials and all three indenters in relation to the reference values. Cube corner results are depicted by triangles, Berkovich results from Nanoindenter XP are depicted by squares and Berkovich results from UMIS-2000 are depicted by spheres. As expected, the results of the reference materials fused silica and sapphire agree well with the reference data because they were used for the calibration of instrument compliance and area function. The scatter of the sapphire data is slightly higher and some of the cube corner results for sapphire are too low. However, a trend in the deviations cannot be seen. This shows that the two materials are suitable for the calibration of the area function of a cube corner tip in the used load range.

The same XP cube corner and Berkovich tips were used for indentation experiments inside a Scanning Electron Microscope (SEM) using a custom-built SEM-Microindenter. More details about this instrument can be found in [15]. Fig. 3 shows indentations with cube corner indenter into sapphire, Ni, W and glassy carbon. Details of these images will be discussed below. Berkovich indentations inside the SEM were done for fused silica and sapphire loads above 700mN (not shown here). No cracks or chipping could be observed in fused silica at 736 mN while cracks along the edges could be seen for a higher force of 1226 mN. In sapphire, the surface around the Berkovich indents was surprisingly smooth. Only cracks starting at the corners could be seen. A cube corner indent into sapphire is shown in Fig. 3a. As expected, the fracture effects are much more pronounced for the cube corner indenter than for the Berkovich tip.

It can be seen in Fig. 2 that there is a good agreement of the modulus results with the reference values for all three indenters for W, Au-Cu alloy and cemented carbide. A clear depth dependence of the result cannot be observed. Pile-up effects do not seem to influence the modulus results markedly. The scatter of the cube corner results is higher than for the Berkovich indenter; however there is no indication that the analysis method cannot be applied for cube corner indentations. The good agreement of the cemented carbide results with the reference value, being by far the material with the highest modulus, indicates that the

instrument stiffness was correctly determined. The Si_3N_4 modulus results of the Berkovich indenter agree well with the reference value of 304 GPa, but the cube corner indenter yields incorrect results. The obtained modulus is significantly lower than the reference value and the discrepancy increases with decreasing load. We attribute this finding to the higher sensitivity of the sharper cube corner tip to the grain size and the brittleness of the ceramic material. Probably the results are affected by cracking effects.

The modulus results for glassy carbon with its high elasticity (the energy release is about 90%) are close to the reference value. The difference for the cube corner indenter is slightly higher but it is not significant. The Ni results for the three indenters agree well, however they are all higher than the reference value. This can be attributed to the marked pile-up effect for this material (see fig. 3d). The contact area derived from the indentation data is therefore too small. W also shows a pile-up effect, however it is less pronounced and seems not to influence the modulus results. Fig. 3g and h shows the crack development in glassy carbon. Radial cracks can be seen at the corners of the indenter and lateral cracks have developed inside the indent, parallel to the surface. The inwards bowing of the edges after unloading is due to the high elasticity of the material and indicates a sink-in effect. Usually a sink-in effect is connected with an overestimation of the contact area and therefore an underestimation of the hardness. However, the hardness results for this material (see below) are rather too high which contradicts this interpretation. The contact area cannot be calculated accurately enough from the load-displacement curve alone as this material does not appear to behave in a manner consistent with conventional contact mechanics.

3.3. Hardness results

The depth dependent hardness results for all investigated materials are shown in Fig. 4. Several effects can be observed. The hardness results are generally not as constant as the modulus results for all tips. The fused silica results obtained with the UMIS Berkovich decreases markedly towards smaller contact depths. This is caused by the large tip radius of 0.84 µm. Measurements at 0.3 mN (first data point) are fully elastic for this tip and the hardness value is only the contact pressure for this load. At higher loads the elastic-plastic transition takes place and only above about 2 mN (third data point) is a fully developed plastic zone established. The cube corner results for fused silica show a slight minimum at medium loads between 5 mN and 10 mN (200 nm – 800 nm depth). The reason for this effect is unknown. Generally the indentation hardness results for fused silica are about 1 GPa higher than the reference values. The difference is less pronounced for smaller loads and sharper tips.

The reason for the higher indentation hardness is the cushion shape of the indents. Other than glassy carbon, fused silica shows the largest inwards bowing of the indentation edges after unloading. This is also the reason for the large radial displacement correction for fused silica (see paragraph 2.4). The indentation area for the calculation of Vickers hardness is overestimated, since it is calculated from the diagonal lengths only. Indentation hardness is therefore a better measure for the plastic properties of fused silica than Vickers hardness and has a closer connection to the real contact pressure.

The hardness results for sapphire agree well with the reference hardness. The large hardness increase at small loads for the blunt Berkovich tip is remarkable. The measurements are fully elastic up to 10 mN load (fourth data point from left). The hardness value in this load range represents only the contact pressure and not the plastic properties of the material. Sapphire reaches here an apparent hardness of 40 GPa, i.e. the theoretical strength of about $1/10^{th}$ of the modulus. A reason for this high strength is the high surface quality and low roughness and the small dimension of the contact area of only $0.23\ \mu m^2$. The probability for the presence of flaws around such a small area is low.

W shows a strong hardness increase towards the surface, which is similar for all three tips. The increase for the rounder Berkovich is smaller. Such a hardness increase towards the surface can also be observed for the other investigated samples Au-Cu alloy and Ni. This effect is often described in the literature as indentation size effect (ISE). In fact the hardness increase cannot be attributed to only one effect. An important feature of the investigated metals is the modification of the grain structure and the work hardening during the cutting and polishing procedure. It is known that mechanical preparation modifies the surface to a depth of some micrometers (see e.g. [25]). Another reason is the required agglomeration of dislocations at the very beginning of the plastic deformation [26]. Gao and Nix have shown that hardness should increase proportional to $1/\sqrt{h}$ in crystalline materials (for sharp conical indenters). Later Qu, Nix et al. [27] have shown that this relation strongly depends on the indenter tip radius. Of course a hardness decrease can be expected in the transition range from elastoplastic to wholly elastic deformation. The measured hardness gradient in the low depth range is therefore inevitably a combination of several effects. According to the model of Qu, the lower hardness increase towards the surface in W for the UMIS data can be attributed to the larger tip radius. Interestingly the difference was not seen in the nickel.

The hardness increase for the Au-Cu alloy can only be seen for the rounder Berkovich tip where data are available from smaller depths. At higher depths there is no difference between the tips and the hardness results agree well with the reference value.

The hardness of Si_3N_4 does not depend on the tip rounding of the Berkovich tip and agrees with the reference value. However, the hardness, measured with the cube corner indenter, is smaller and decreases towards the surface. Analogous to the modulus results, the sharper indenter seems to be more sensitive to the grain size and brittleness of the ceramics. The opposite effect can be observed for cemented carbide. While the hardness results for both Berkovich tips agree very well with each other and with the reference value, a hardness increase is seen for the cube corner indenter. The analysis of this effect is outside the scope of this investigation.

The hardness results for glassy carbon show differences between all three indenters, especially at small loads. The apparent hardness is higher the sharper the tip is. This effect was not investigated in detail. Possibly it has to do with crack formation in the material as can be seen in Fig. 3h. More investigations are needed for an understanding of this effect.

The hardness results for Ni do not show significant differences between the indenters. There is a strong hardness increase towards the surface which reaches nearly two times the bulk value. The reference value is only reached for the highest loads at a depth of more than 3 µm. A pile-up effect increases the contact area and the calculated area value from the load-displacement curve is too small and leads to a higher apparent hardness.

Summarizing the results of all materials it can be stated, that there is no general hardness difference seen for the indenters with different tip angle. Hardness results were found to be similar for metals, glass and sapphire. Significant differences occur for the ceramic materials and the highly elastic glassy carbon. Some of the differences at small loads can be attributed to the different tip rounding and to the tip angle.

Hardness is contact pressure under load for a fully developed plastic zone. If such a zone can not develop due to severe cracks or very high elasticity of the material, hardness may no longer be a reasonable measure for the plastic properties of the material.

Although the maximum strain below the indenter is larger for a smaller face angle, the contact pressure represents an average of the whole strain field. As mentioned in the introduction, hardness is related to the yield stress Y in simple compression over the constraint factor C. Tabor [13] has shown that the results for a perfectly plastic solid may be applied for a strain-hardening solid if the flow stress for a representative strain ε_R is used with

$$\varepsilon_R \approx 0.2 \cdot \tan\beta \tag{6}$$

The representative strain is 8% for Vickers and Berkovich indenter and 18% for a cube corner indenter. This representative strain should decrease if the material is already work hardened e.g. mechanically polished metal surfaces to a depth of a few micrometers. The constraint

factor for metals is then close to three, independent of the indenter angle. Johnson [11, pp.163] has shown that the dependency of the contact pressure (hardness) on the indenter angle is further reduced with increasing friction coefficient. Metals have a higher friction coefficient against diamond than the other investigated materials (typically 0.15 – 0.25). This may explain why a significant hardness difference between the different indenters was not observed for the metal samples.

4. Conclusions

Indentation measurements with Berkovich and cube corner indenters were carried out on eight different materials with two different commercial nanoindentation instruments over a load range between 0.3 mN and 500 mN. The hardness and modulus results were compared with reference values obtained by different methods.

It has been shown that the instrument stiffness can be determined by a comparison of two area functions obtained using fused silica and sapphire as reference materials. The accuracy of the area function calculation could be improved by considering additionally the elastic radial displacement within the contact area. This is especially important if fused silica is used as reference material because it requires the largest correction.

The modulus results for fused silica, sapphire and glassy carbon show that the unloading fit range has a much bigger influence on the results for the cube corner indenter than for the Berkovich tip. Fused silica and glassy carbon have a characteristic kink in the unloading curve independent of the maximum load. Therefore the unloading curves of a cube corner indenter should be carefully inspected to ensure smooth curvature and the unloading fit range has to be chosen warily to enable a reliable comparison of the results. A fit range of less than 50% is recommended.

A comparison of the modulus results has shown that there is no significant difference between the results from different instruments or between cube corner and Berkovich indenters. This confirms that the same calibration procedures can be applied, independent of the indenter shape. Further, the indentation modulus results agree well with the reference values obtained by other methods. A good agreement with the Young's modulus reference value of the very stiff cemented carbide confirms the correctness of the calculated instrument compliance, since an error in the compliance correction would have the highest influence on results from this

material. Cracks in sapphire and fused silica, which evolve mainly in the upper load range, had no noticeable influence on the modulus results.

The hardness comparison has shown that for the majority of the investigated materials, there is no fundamental hardness difference for indenters with different tip angles. This means that the contact pressure below the indenter is approximately equal after development of the full plastic zone. The difference between Berkovich and cube corner indenter increases with decreasing contact depth. Some of the differences at small loads can be attributed to the different tip rounding. Materials like silicon nitride, cemented carbide or glassy carbon, however, show a clear deviation from the hardness reference value for the cube corner indenter although the modulus difference is not so much pronounced. Deviations are equally possible above as below the reference value. The reasons for the deviations were not studied in detail. In the case of silicon nitride the brittleness of the material seems to result in a micro-crack enhancement for the sharper tip and therefore in a hardness decrease. For cemented carbide the hard WC particles in the softer cobalt matrix seem to determine the total response of the compound more for a sharper tip. The slip-line theory (see [9]) of metal forming cannot be applied for these materials.

Generally the scatter of the results is larger for the sharper cube corner tip. Therefore Berkovich indenters should be preferred for comparable hardness and modulus results. Cube corner indenters require a careful calibration but can then be used, for instance as an additional tip for the evaluation of the stress-strain relation of plastic materials.

Acknowledgements

Table 1:

Hardness and modulus results obtained with different tips and instruments as an average of all measurements with different maximum load. ΔH is the standard deviation of 10 measurements at 500mN for the reference measurements. For the indentation measurements ΔH and ΔE are the standard deviations of the results of all loads for one sample without including the scatter of the ten measurements averaged at each load. Hardness results below 40 nm indentation depth are not included in the average.

Hardness in GPa	Reference		UMIS Berkovich		XP Berkovich		XP Cube corner	
	H	ΔH	H	ΔH	H	ΔH	H	ΔH
Fused silica	7.5	0.1	8.8	0.3	8.1	0.6	8.4	0.7
Sapphire	23.6	1.1	22.5	2.2	21.6	1.3	22.2	1.2
W	5.39	0.17	5.9	1.0	6.5	1.6	6.4	1.7
Au-Cu alloy	2.53	0.05	2.65	0.22	2.32	0.05	2.24	0.15
Si_3N_4	19.5	2.3	19.0	1.0	17.7	0.6	16.1	2.3
Cem. Carbide	30.1	1.5	29.1	1.8	28.4	1.4	36.4	5.4
Glassy carbon	3.9	0.4	3.8	0.24	4.6	0.3	4.9	0.7
Ni	1.63	0.04	2.7	0.4	2.3	0.7	2.1	0.4
E-Modulus in Gpa	E		E	ΔE	E	ΔE	E	ΔE
Fused silica	72		71.5	1.9	71.5	0.8	72.2	0.8
Sapphire	420		430.8	10.2	415.9	7.3	401.5	19.0
W	410		413.8	25.5	414.6	33.8	394.4	36.2
Au-Cu alloy	93		98.9	4.2	90.5	1.1	100.6	4.6
Si_3N_4	304		299.9	6.3	293.4	3.7	260.2	22.2
Cem. Carbide	654		642.4	24.5	621.4	16.4	614.6	38.1
Glassy carbon	27		25.9	0.2	27.2	1.1	25.5	1.2
Ni	200		227.0	19.3	226.6	9.2	241.0	5.5

List of Figure Captions

Figure 1:

Indentation modulus of **(a)** fused silica 500mN maximal load; **(b)** sapphire 100mN maximal load, and, **(c)** glassy carbon 500 mN maximal load, determined as a function of the unloading fit range for a Berkovich (squares) and a cube corner (triangles) tip. The measurements have been done with a MTS Nanoindenter XP. The horizontal solid line indicates the reference modulus value.

Figure 2:

Contact depth dependent modulus results for the investigated materials measured with UMIS Berkovich (circles), XP Berkovich (squares), and XP cube corner (triangles). The horizontal solid lines indicate the reference modulus values.

Figure 3:

In-situ SEM indentations in sapphire (a, b) at 981 mN, Ni (c, d) at 343 mN, W (e, f) at 981 mN and glassy carbon (g, h) at 343 mN using a cube corner with the SEM-Microindenter. The left column shows the indented material close to or at maximum load and the right column the residual indent. Note the pronounced pile-up around the indent for Ni and W.

Figure 4:

Contact depth dependent indentation hardness for all investigated materials measured with UMIS Berkovich (circles), XP Berkovich (squares), and XP cube corner (triangles). The horizontal solid lines indicate the reference hardness values.
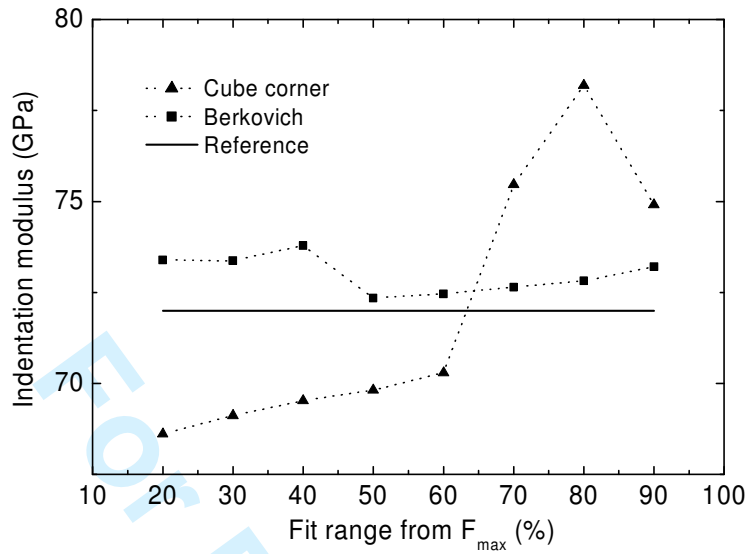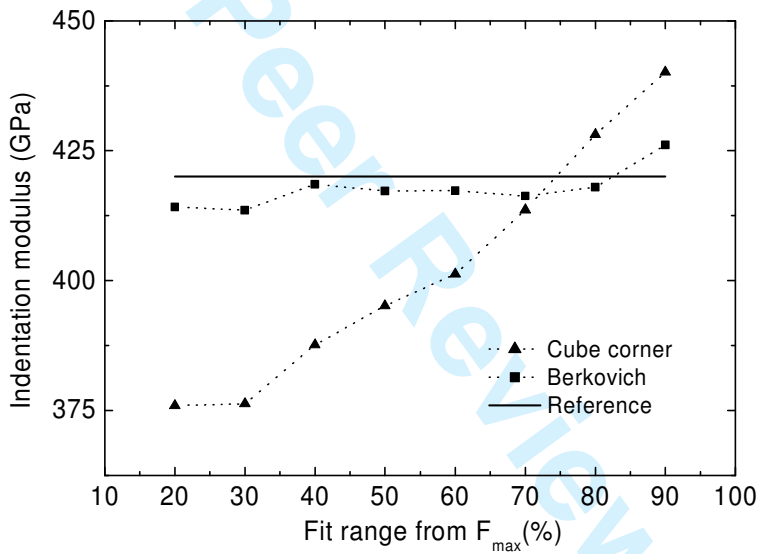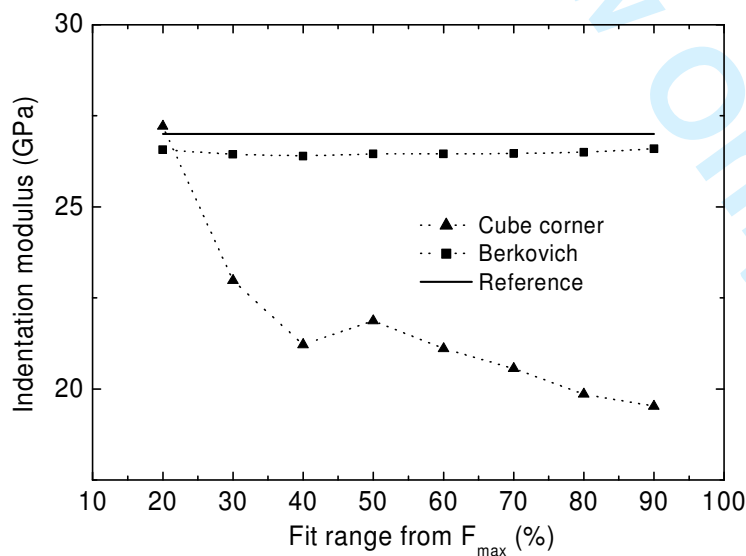
Fig. 1
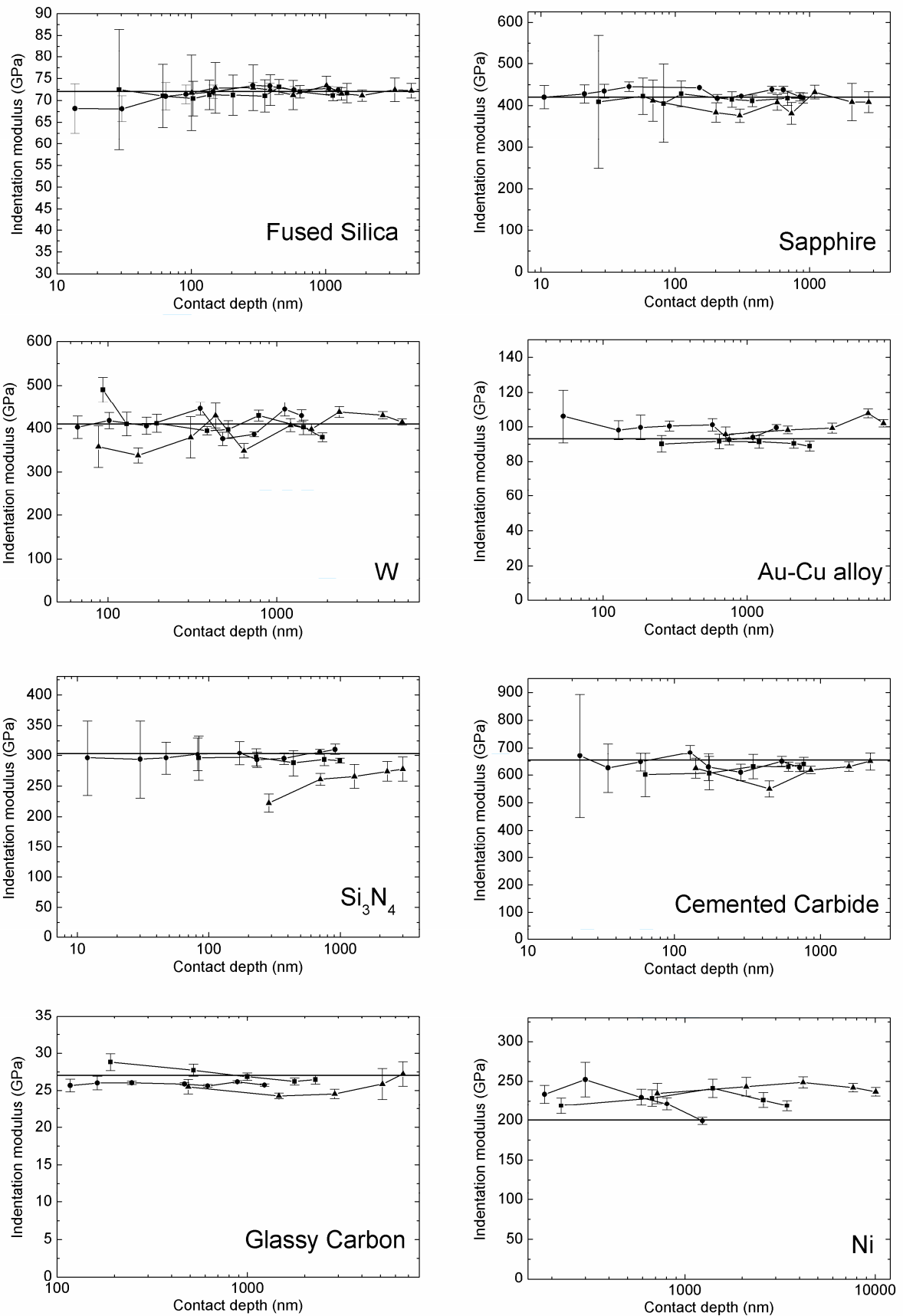
Fig. 2
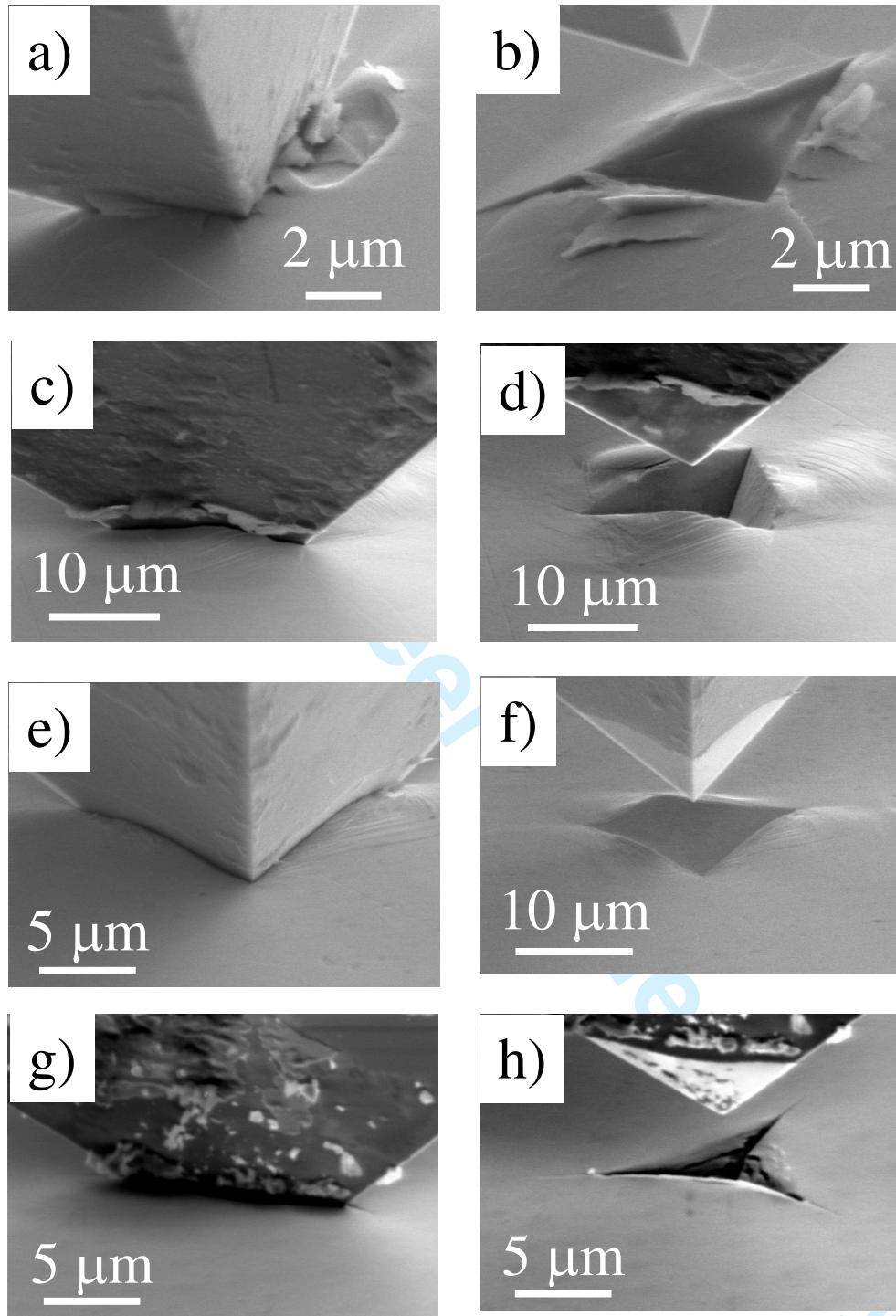
Fig. 3
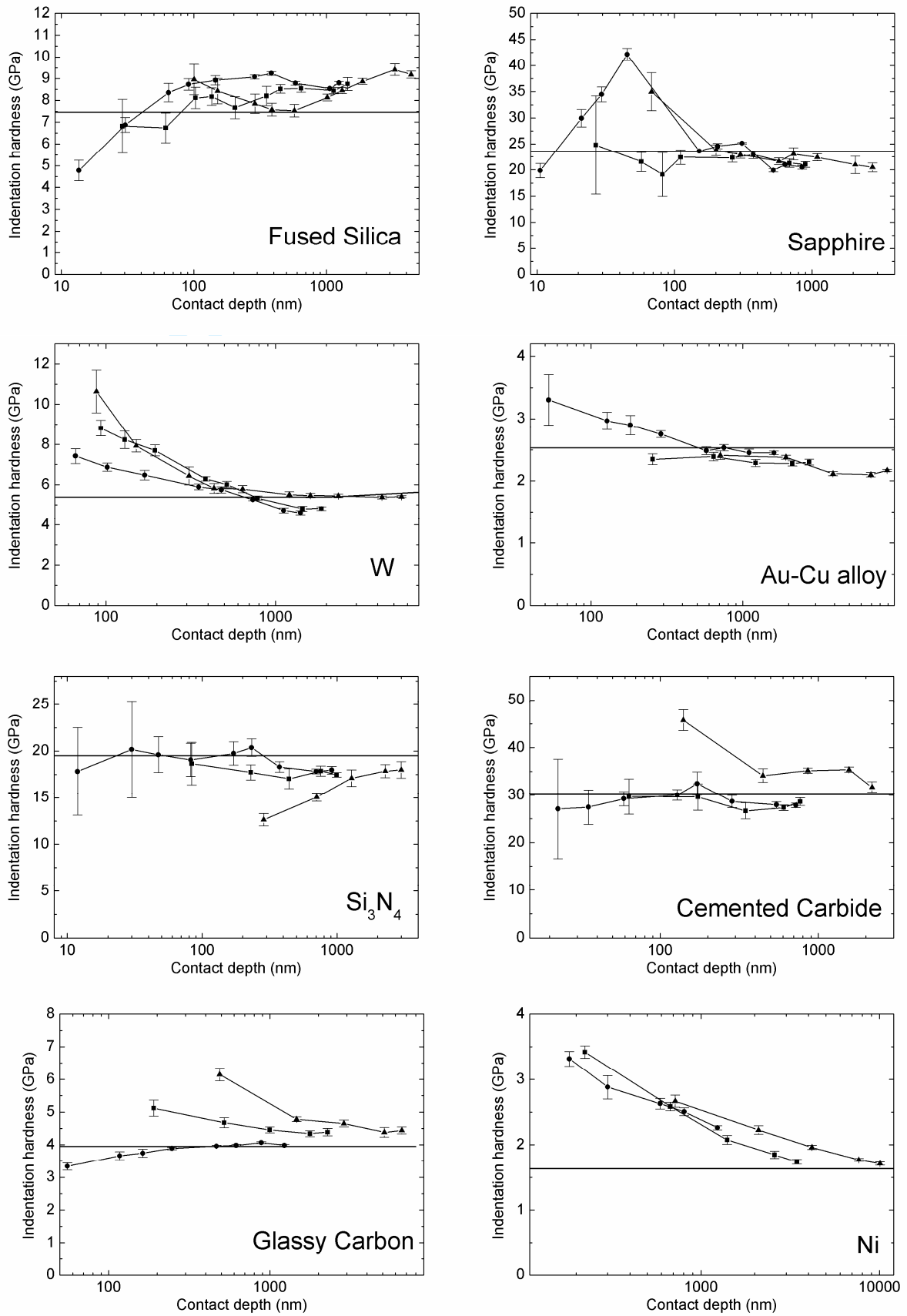
Fig. 4

References

[1]   C.B. Ponton, R.D. Rawlings, Vickers indentation fracture toughness test, Part 1 and 2, Mat. Sci. and Technol. 5, 865-976 (1989).

[2]   D.S. Harding, W.C. Oliver, G. M. Pharr, Cracking during nanoindentation and its use in the measurement of fracture toughness, Mat. Res. Soc. Symp. Proc. 356, 663-668 (1995).

[3]   S. Stauss , P. Schwaller , J.-L. Bucaille , R. Rabe , L. Rohr , J. Michler, E. Blank, Determining the stress–strain behaviour of small devices by nanoindentation in combination with inverse methods, Microelectronic Engineering 67–68, 818–825 (2003).

[4]   J.L. Bucaille, S. Stauss, E. Felder, J. Michler, Determination of plastic properties of metals by instrumented indentation using different sharp indenters, Acta Materialia 51, 1663 (2003).

[5]   J.-L. Bucaille, S. Stauss , P. Schwaller , J. Michler, A new technique to determine the elastoplastic properties of thin metallic films using sharp indenters, Thin Solid Films 447-448, 239-245 (2004).

[6]   N. Chollacoop, M. Dao, S. Suresh, Depth-sensing instrumented indentation with dual sharp indenters, Acta Materialia 51, 3713–3729 (2003).

[7]   J. S. Field, M. V. Swain, R. D. Dukino, Determination of fracture toughness from the extra penetration produced by indentation-induced pop-in, J. Mater. Res. 18, 1412-1419 (2003).

[8]   W.C. Oliver, G.M. Pharr, J. Mater. Res. 7, 1564-1583 (1992).

[9]   R. Hill, The Mathematical Theory of Plasticity, (Clarendon Press, Oxford, 1950).

[10] D.M. Marsh, Plastic flow in glass, Proc. R. Soc. London, A279, 420-435 (1964).

[11] K.L. Johnson, Contact Mechanics, (Cambridge University Press, Cambridge, 1985).

[12] J. Zhang, M. Sakai, Geometrical effect of pyramidal indenters on the elastoplastic contact behaviors of ceramics and metals, Materials Science and Engineering A 381, 62-70 (2004)

[13] D. Tabor, Hardness of Metals, Oxford, University Press (1951)

[14] ISO 14577, Metallic materials – Instrumented indentation test for hardness and materials parameters, 2002, ISO Central Secretariat, 1211 Geneva 20, Switzerland.

[15] R. Rabe, J.-M. Breguet, P. Schwaller, S. Stauss, F.-J. Haug, J. Patscheider and J. Michler, Observation of fracture and plastic deformation during indentation and scratching inside the scanning electron microscope, Thin Solid Films, 469-470, 206-213 (2004)

[16] European project, EC Contract G6RD-CT2000-00418 "Certified Reference Materials for Depth Sensing Indentation Instruments 'DESIRED'

[17] European project: Determination of Hardness and Modulus of Thin Films and Coatings by Nanoindentation (INDICOAT), contract no. SMT4-CT98-2249, NPL Report MATC(A) 24, May 2001.

[18] Tables of Physical and Chemical Constants, Ed. W. G.C. Kaye, T.H. Laby, (Longman, London, 1995).

[19] T. Chudoba, M. Griepentrog, A. Dück, D. Schneider, F. Richter, Young's modulus measurements on ultra-thin coatings, J. Mater. Res. 19, 301-314 (2004).

[20] W.C. Oliver, G.M. Pharr, Measurement of hardness and elastic modulus by instrumented indentation: Advances in understanding and refinements to methodology, J. Mater. Res. 19, 3-20 (2004).

[21] R.B. King, Elastic analysis of some punch problems for a layered medium, Int. J. Solids Structures 23 no. 12, 1657-1664 (1987).

[22] M.T. Hendrix, The use of shape correction factors for elastic indentation measurements, J. Mater. Res. 10, 255-258 (1995).

[23] J. B. Wachtman Jr., W.E. Tefft, D.G. Lam Jr., R.P. Stinchfield, Elastic constants of synthetic single crystal corundum at room temperature. J. Res. Nat. Bur. Stand. A. Physics and Chemistry 64A, 213–228 (1960).

[24] J. J. Vlassak, M. Ciavarella, J. R. Barber, X. Wang, The indentation modulus of elastically anisotropic materials for indenters of arbitrary shape, Journal of the Mechanics and Physics of Solids, 51, 1701 – 1721 (2003).

[25] Y. Liu, A.H.W. Ngan, Depth Dependence of Hardness in Copper Single Crystals Measured by Nanoindentation, Scripta Mater 44, 237-241 (2001).

[26] W.D. Nix, H. Gao, Indentation size effects in crystalline materials: a law for strain gradient plasticity, J. Mech. Phys. Solids 46, 411-425 (1998).

[27] S. Qu, Y, Huang, W.D. Nix, H. Jiang, F. Zhang, K.C. Hwang, Indenter tip radius effect an the Nix-Gao relation in micro- und nanoindentation hardness experiments, J. Mater Res. 19, 3423-3434 (2004)
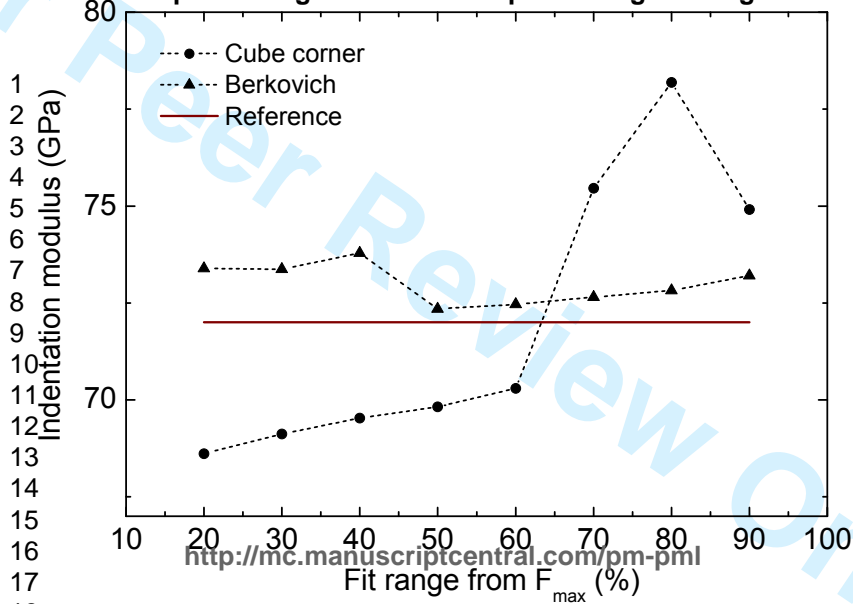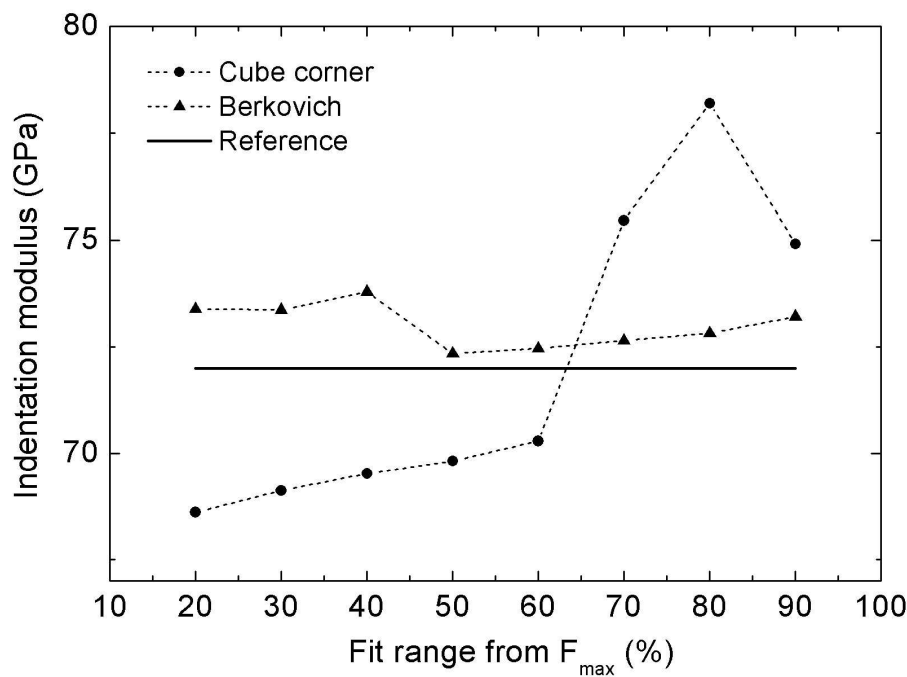
Figure 1(a)
300x232mm (150 x 150 DPI)
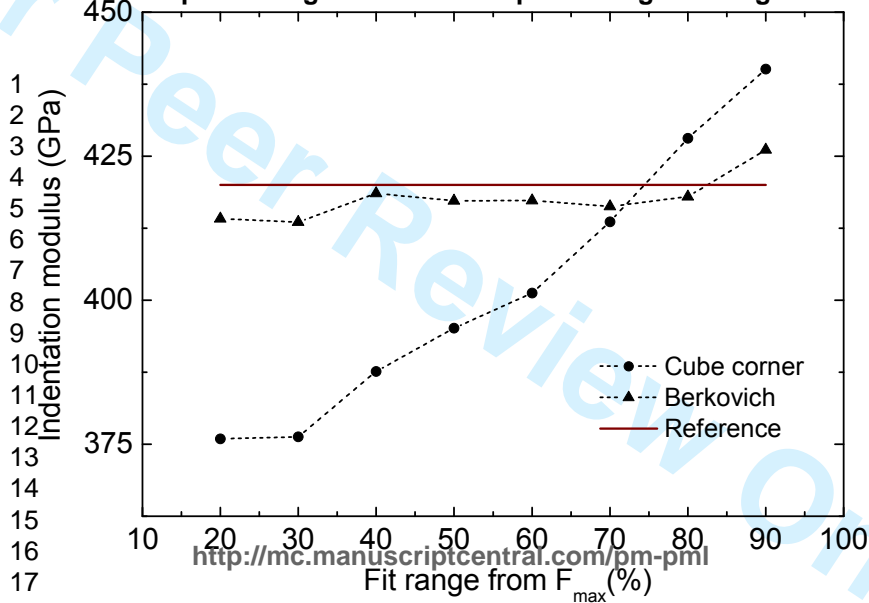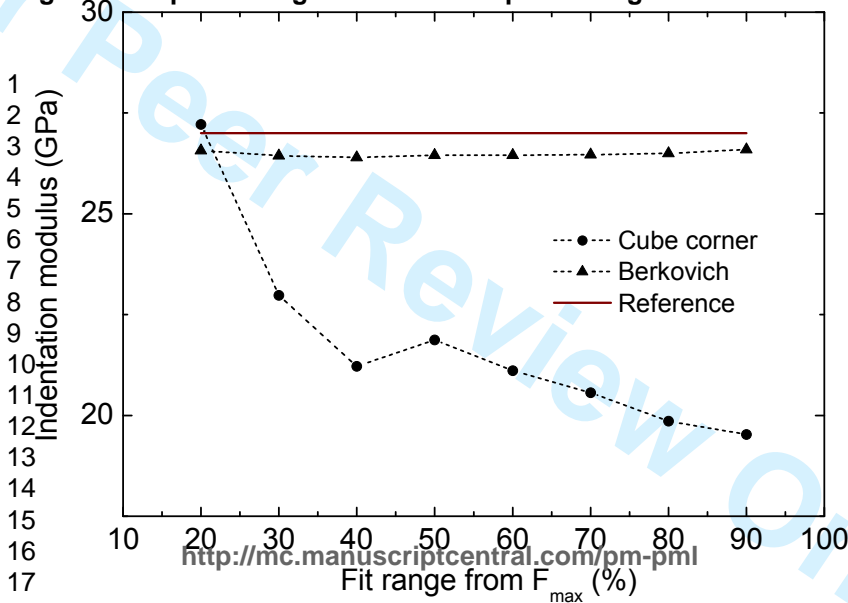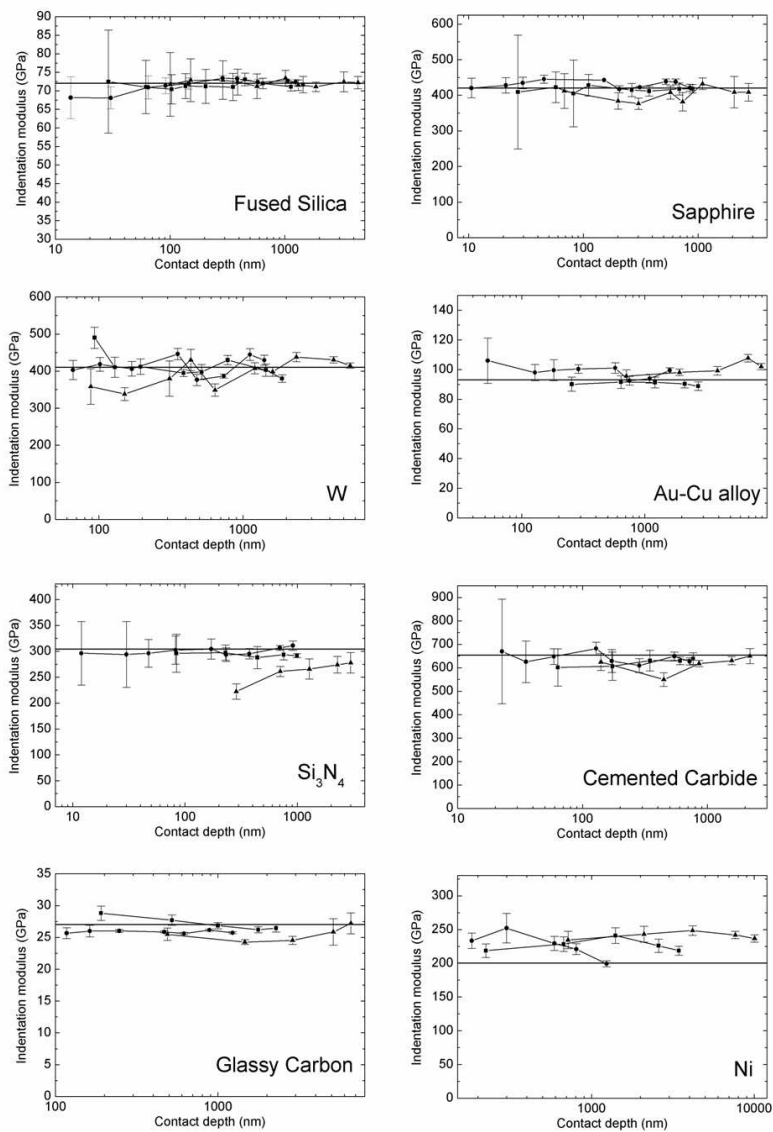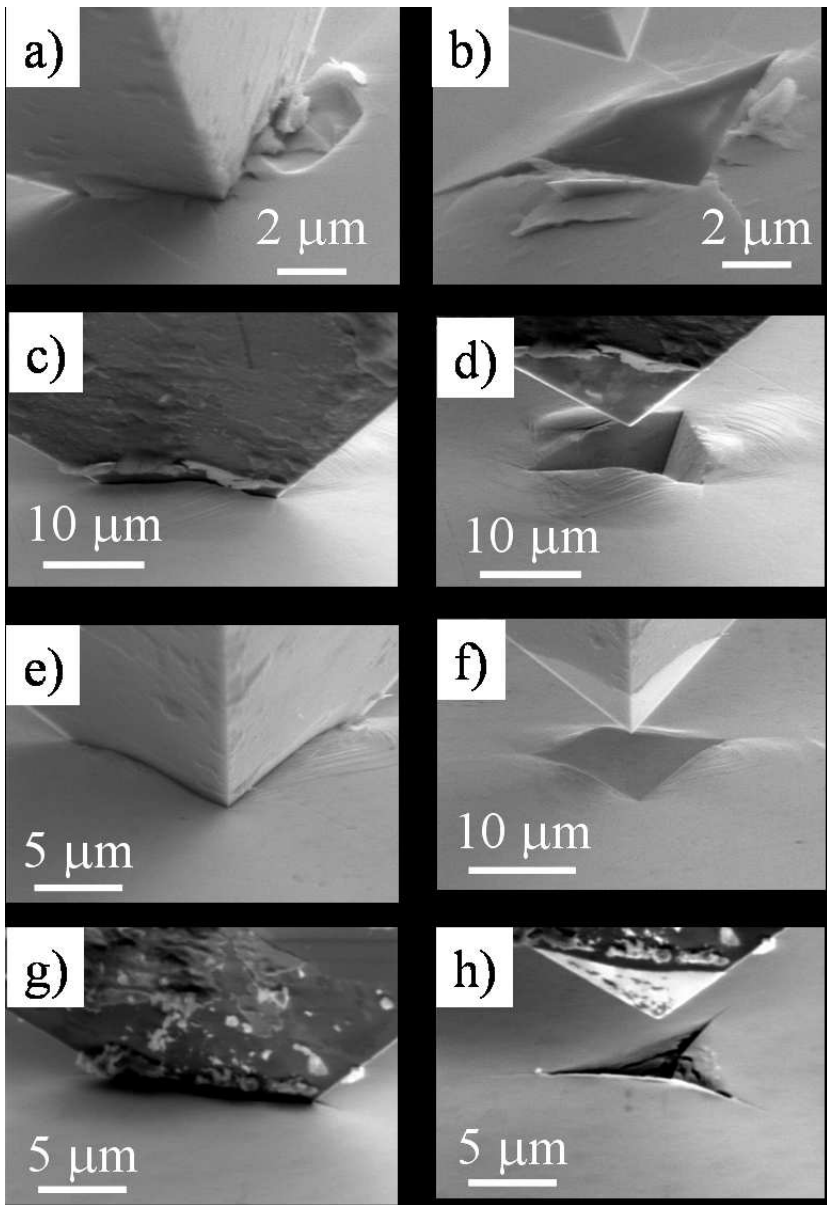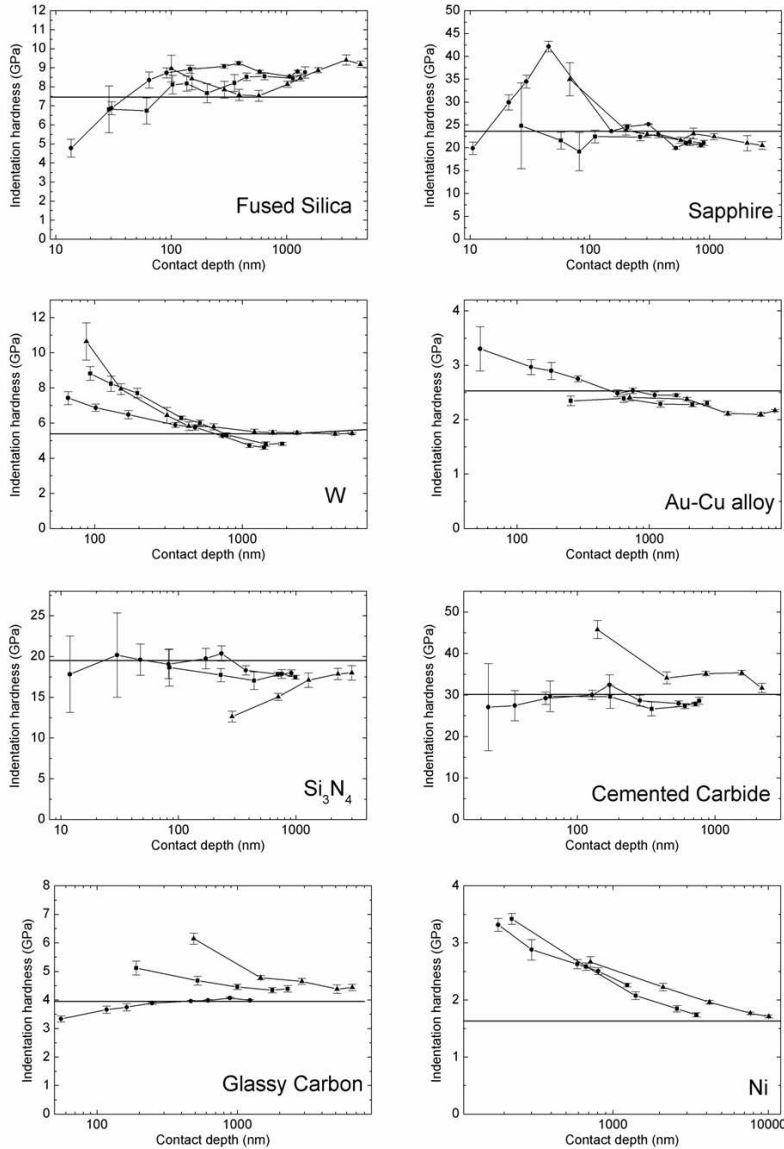
Figure 2
170x241mm (150 x 150 DPI)

Figure 3
131x190mm (150 x 150 DPI)

Figure 4
163x236mm (150 x 150 DPI)